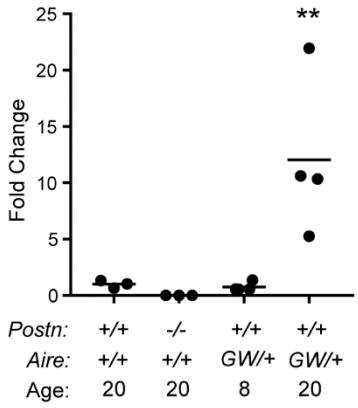

Supplemental figure 1: *Postn* is upregulated in neuropathic compared to pre-neuropathic *NOD.Aire*$^{GW/+}$ mice. *Postn* expression in *NOD.WT* mice, *Postn*$^{-/-}$ mice and *NOD.Aire*$^{GW/+}$ mice at different ages. *Postn* expression was measured by qPCR in 20-week-old *NOD.WT*, 20-week-old *B6.Postn*$^{-/-}$, 8-week-old (pre-neuropathic) *NOD.Aire*$^{GW/+}$, and 20-week-old *NOD.Aire*$^{GW/+}$ mice. Values are represented as fold change over *NOD.WT*. Each dot represents an individual animal. **p<0.005 by ordinary one-way ANOVA with Tukey's test for multiple comparisons.

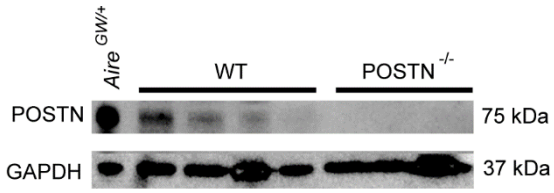

Supplemental figure 2: POSTN protein is absent in *NOD.Postn$^{-/-}$* mice. POSTN expression was measured by Western blot from sciatic nerve lysates from *NOD.Aire$^{GW/+}$* neuropathic, *NOD.WT* (WT), and *NOD.Postn$^{-/-}$* mice. GAPDH was used as a loading control. Each lane represents an individual mouse.

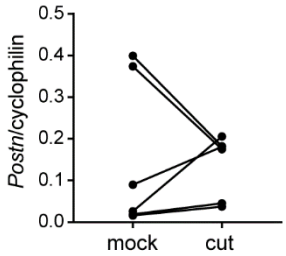

Supplemental figure 3: *Postn* expression is unaltered in nerve transection. The sciatic nerve of *B6* mice was transected (cut) or exposed but left intact (mock). Three days following nerve transection surgery, RNA was isolated from sciatic nerve and *Postn* was measured by qPCR. Each dot represents an individual mouse. Lines connect mock and cut samples from the same mouse. p=0.32 by paired T test.

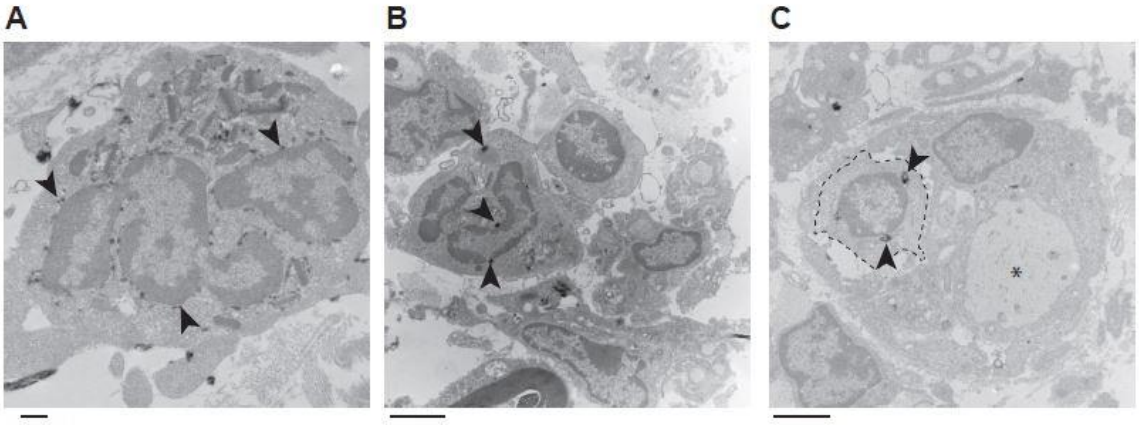

Supplemental figure 4: *Postn* is expressed by non-Schwann cells. Histochemistry for beta-galactosidase using X-gal was performed on sciatic nerves from *NOD.SCID.Postn*$^{lacZ/+}$ reporter mice with AT of *NOD.Aire*$^{GW/+}$ splenocytes and nerves were imaged with electron microscopy. Arrowheads indicate X-gal crystals, which are electron-dense. * indicates axons. The dotted line indicates a cell outline. X-gal crystals are found in the nuclear membrane of cells that lack a basal lamina (A, B), and cells that have crossed the Schwann cell basal lamina but do not associate with an axon (C).

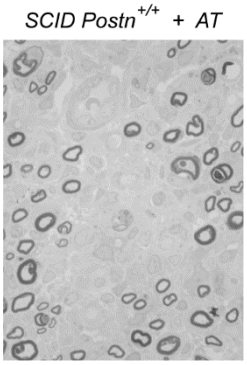

Supplemental figure 5: X-gal crystals are specific to the *lacZ* transgene. Semi-thin section (stained with paraphenylenediamine) of a *NOD.SCID.Postn*$^{+/+}$ adoptively transferred with *NOD.Aire*$^{GW/+}$ splenocytes. X-gal crystals are absent.

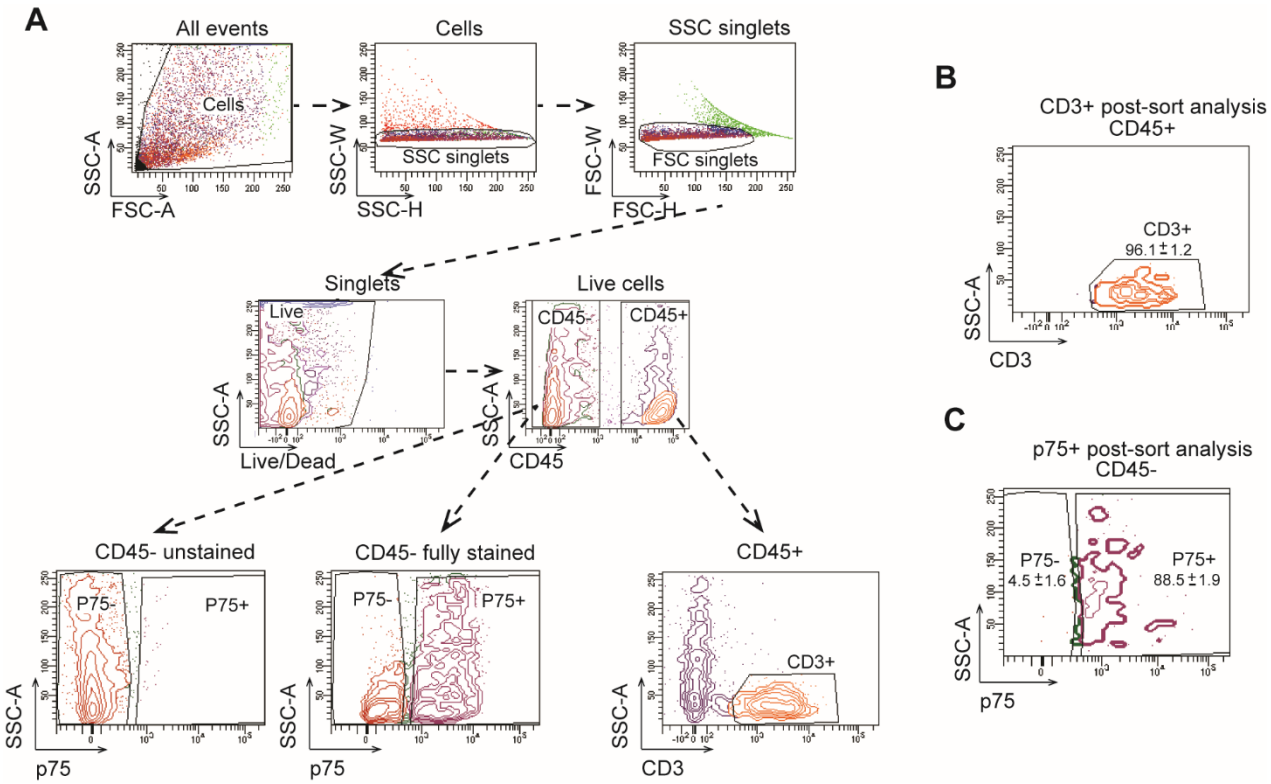

Supplemental figure 6: Gating strategy for isolation of p75+ Schwann cells from SAPP mice. A) Diagram of the gating strategy used to isolate live, CD45- p75+ Schwann cells from sciatic nerve of neuropathic *NOD.Aire*$^{GW/+}$ mice. First, debris was excluded by drawing a large gate on forward scatter (FSC) area (A) versus side scatter (SSC)-A labelled “Cells”. Next doublets were excluded by drawing a gate around singlets on SSC height (H) versus width (W) followed by drawing a gate around singlets on FSC height versus width. Next, dead cells were excluded and CD45 was used to distinguish hematopoietic cells from nerve-resident cells. Within the CD45- gate, p75+ cells were identified using an “unstained” control in which the sample included all dyes and antibodies in the stain set except anti-p75. Within the CD45+ gate, CD3+ T cells were identified and collected for use as a negative control for *Postn* expression. B) Representative plot showing the CD3 post-sort purity. The plot was pregated on CD45+ events as shown in A. C) Representative plot showing p75 post-sort purity. The plot was pregated on CD45- events as shown in A. numbers represent the average frequency and standard deviation of events within the gate.

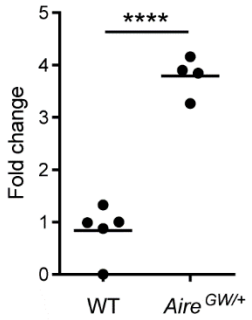

Supplemental figure 7: *Tgfb* is highly expressed in sciatic nerves during SAPP. *Tgfb* expression was measured in sciatic nerve of *NOD.WT* and *NOD.Aire*$^{GW/+}$ neuropathic mice by qPCR. Each dot represents an individual mouse. ****p<0.0001 by two-tailed T test.

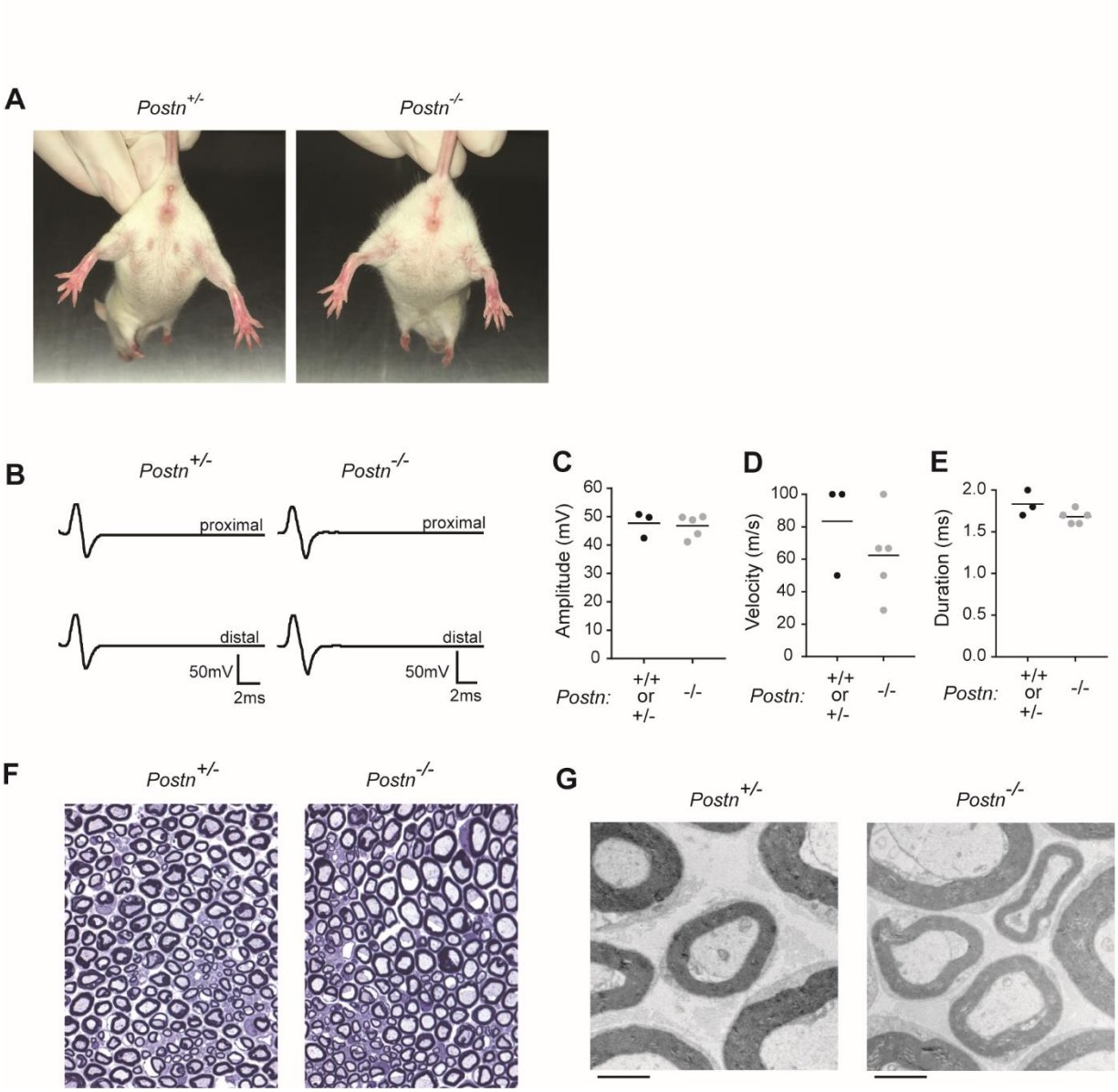

Supplemental figure 8: *Postn* deficient mice have normal peripheral nerves. A) Clinical evaluation of *NOD.Postn*$^{+/-}$ and *NOD.Postn*$^{-/-}$ mice. Normal mice will extend their hind limbs to the side when lifted by the tail, whereas neuropathic animals are unable to do so. B) Representative CMAPs of *NOD.Postn*$^{+/-}$ and *NOD.Postn*$^{-/-}$ mice. *NOD.Postn*$^{-/-}$ and *NOD.Postn*$^{+/-}$ mice had similar CMAP peak amplitudes (C, p=0.99), CMAP durations (D, p=0.99), and conduction velocities (E, p=0.63). Each dot represents an individual animal. Light (F) and electron microscopy (G) of semi-thin and thin sections, respectively, revealed no abnormalities of *NOD.Postn*$^{-/-}$ sciatic nerves. F) Original magnification 100x. G) Scale bar is 2 µm. P-values were calculated using two-tailed, unpaired t tests.

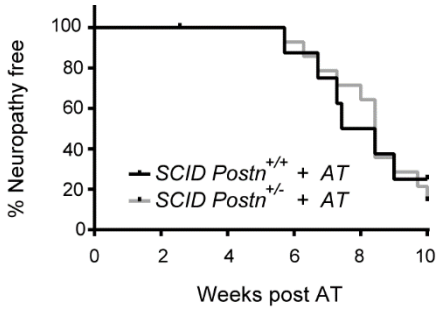

Supplemental figure 9: *NOD.SCID Postn*$^{+/+}$ and *NOD.SCID Postn*$^{+/-}$ mice develop neuropathy at the same incidence. Neuropathy incidence curve showing onset of disease in *NOD.SCID Postn*$^{+/+}$ and *NOD.SCID Postn*$^{+/-}$ mice. p=0.95 by log-rank test.

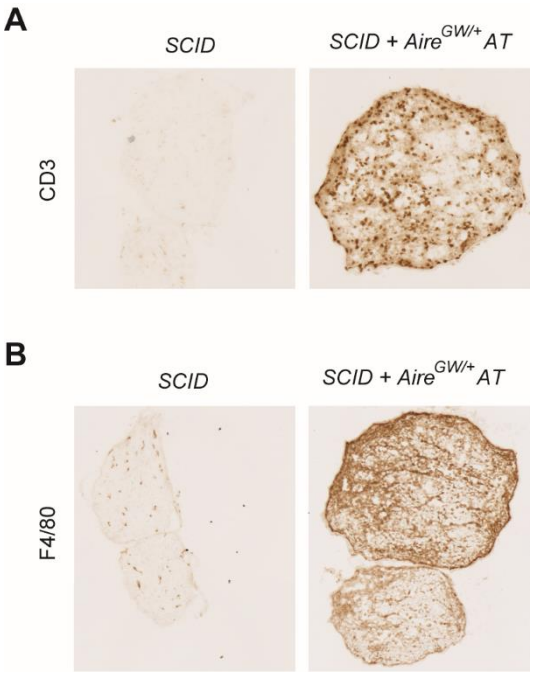

Supplemental figure 10: T cells and macrophages infiltrate the sciatic nerve of adoptively transferred mice. A) CD3, and B) F4/80 immunohistochemical staining of sciatic nerve from *NOD.SCID* mice without and with AT of *NOD.Aire*$^{GW/+}$ splenocytes. Mice with and without AT were processed in parallel.

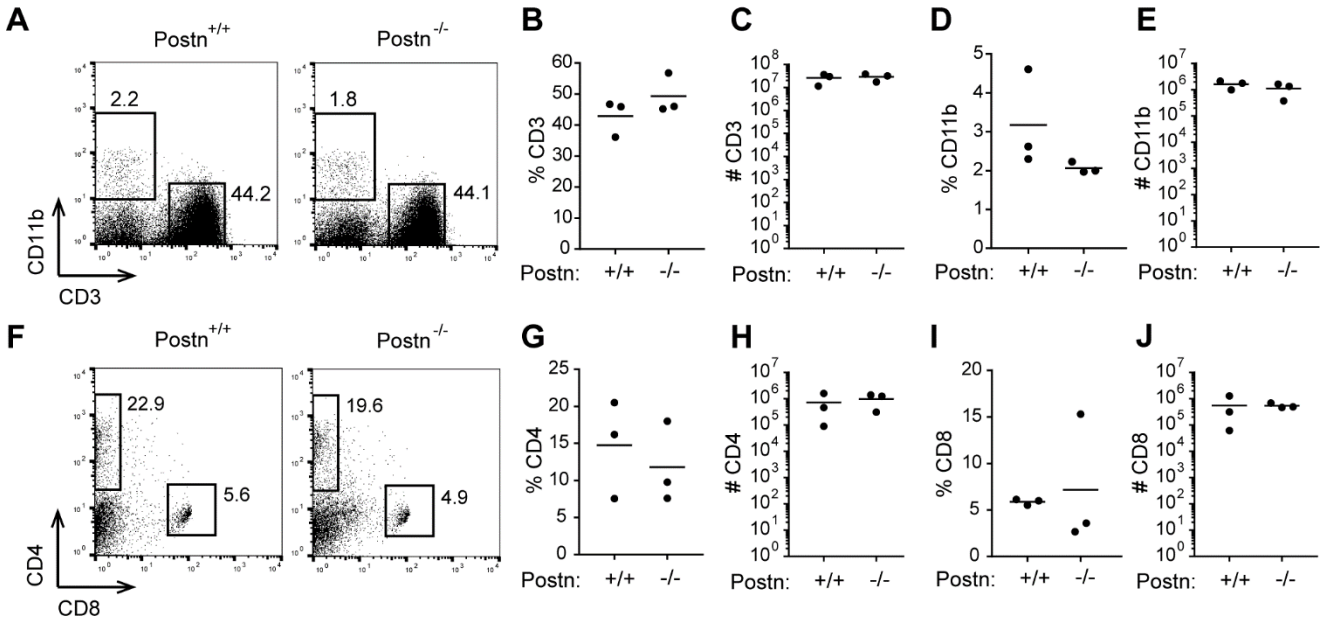

Supplemental figure 11: T cell and macrophage numbers are similar in *NOD.Postn*$^{+/+}$ and *NOD.Postn*$^{-/-}$ mice. A) Representative dot plots showing CD3 versus CD11b staining on splenocytes from *NOD.Postn*$^{+/+}$ and *NOD.Postn*$^{-/-}$ mice. Frequency (B, D) and total numbers (C, E) of CD3+ T cells (B, C) and CD11b+ macrophages (D, E). F) Representative dot plots showing CD8 versus CD4 staining of *NOD.Postn*$^{+/+}$ and *NOD.Postn*$^{-/-}$ mice. Frequency (G, I) and total number (H, J) of CD4+ (G, H) and CD8+ (I, J) T cells. Representative plots are pre-gated on live singlets. Numbers represent the frequency of events in the gate. Each dot is an individual animal. P-values were calculated by two-tailed, un-paired T test.

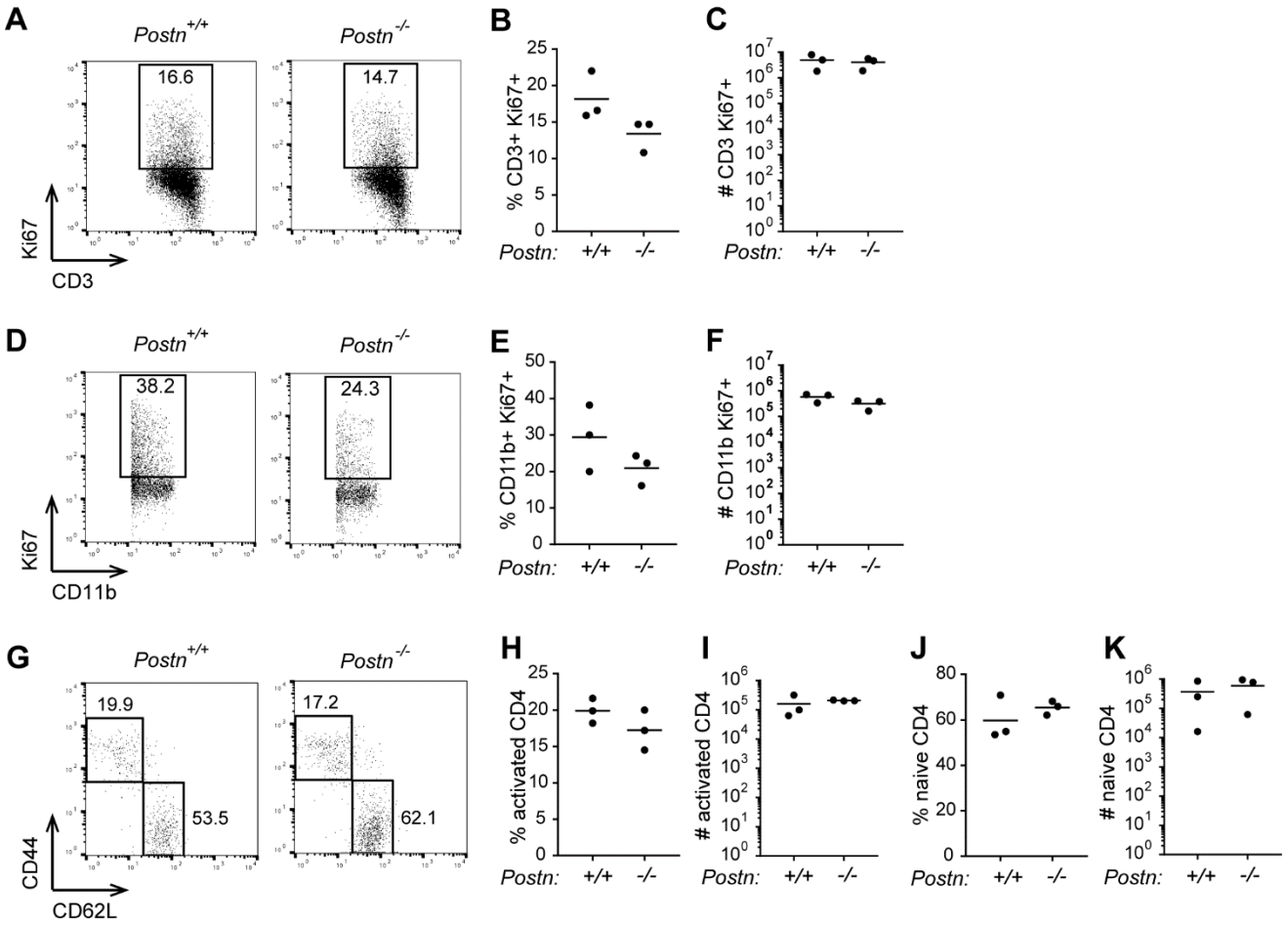

Supplemental figure 12: T cell and macrophage proliferation and/or activation are similar in *NOD.Postn*$^{+/+}$ and *NOD.Postn*$^{-/-}$ mice. A) Representative dot plots showing Ki67 staining on CD3+ T cells from spleen of *NOD.Postn*$^{+/+}$ and *NOD.Postn*$^{-/-}$ mice. Plots are pre-gated on live CD3+ events. Frequency (B) and total number (C) of Ki67+ T cells. D) Representative dot plots showing Ki67 staining on CD11b+ macrophages from spleen of *NOD.Postn*$^{+/+}$ and *NOD.Postn*$^{-/-}$ mice. Plots are pre-gated on live CD11b+ events. Frequency (E) and total number (F) of Ki67+ macrophages. G) Representative dot plots showing CD62L versus CD44 staining on CD4+ T cells from spleen of *NOD.Postn*$^{+/+}$ and *NOD.Postn*$^{-/-}$ mice. Frequency (H, J) and total number (I, K) of activated (CD44+ CD62L-, H, I) and naïve (CD44- CD62L+, J, K) CD4+ T cells. Numbers represent the frequency of events in the gate. Each dot is an individual animal. P-values were calculated by two-tailed, un-paired T test.

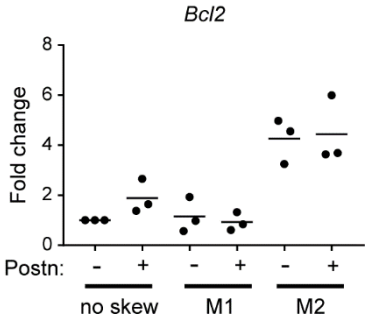

Supplemental figure 13: POSTN does not alter survival. Bone marrow-derived macrophages were skewed in vitro toward an inflammatory M1 or anti-inflammatory M2 phenotype in the presence or absence of 100 ng/ml POSTN. *Bcl2* expression was measured by qPCR. Each dot represents macrophages isolated from an individual animal. P-values were calculated by one-way ANOVA.

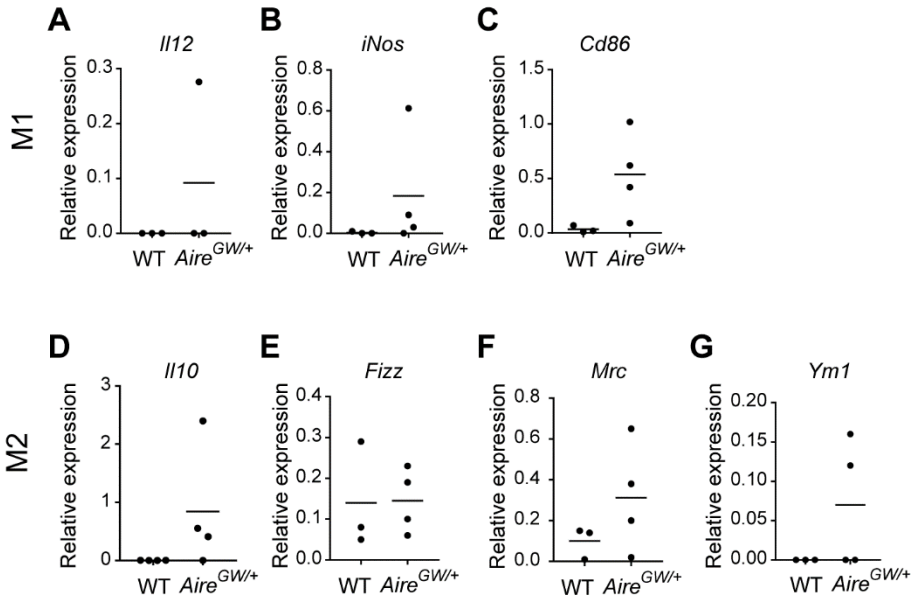

Supplemental figure 14: Nerve infiltrating macrophage phenotype. RNA was isolated from the sciatic nerves of *NOD.WT* (WT) or CD3- CD11b+ macrophages enriched from sciatic nerve of *NOD.Aire*$^{GW/+}$ neuropathic mice. *Il12* (A), *iNos* (B), *Cd86* (C), *Il10* (D), *Fizz* (E), *Mrc* (F), and *Ym1* (G) expression relative to cyclophilin was measured by qPCR. Each dot represents an individual animal. P-values were calculated by two-tailed T test with Welch's correction.

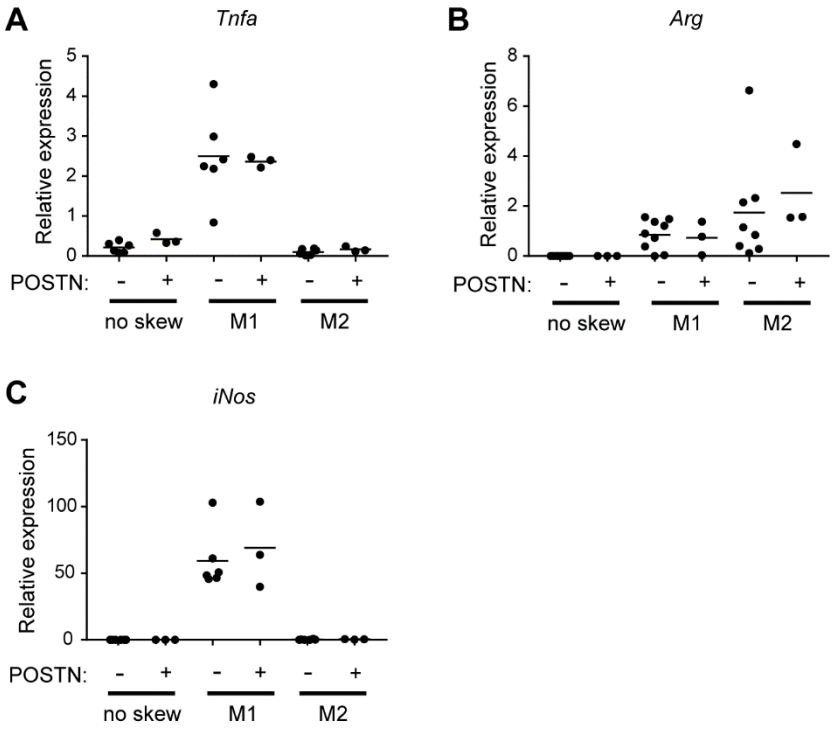

Supplemental figure 15: POSTN does not alter macrophage polarization. Bone marrow-derived macrophages were skewed in vitro toward an inflammatory M1 or anti-inflammatory M2 phenotype in the presence or absence of 100 ng/ml POSTN. *Tnf* (A), *Arg* (B), and *iNos* (C) expression was measured by qPCR. Each dot represents macrophages isolated from an individual animal. P-values were calculated by one-way ANOVA.

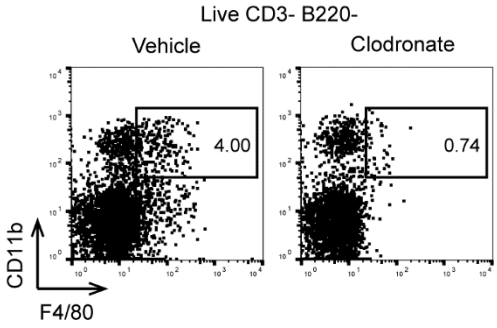

Supplemental figure 16: Clodronate effectively depletes macrophages. *NOD* mice were treated with liposomes containing vehicle or clodronate. Three days post-treatment, splenocytes were isolated and stained for flow cytometry. CD11b+ F4/80+ macrophages were depleted in clodronate-treated compared to vehicle-treated mice.

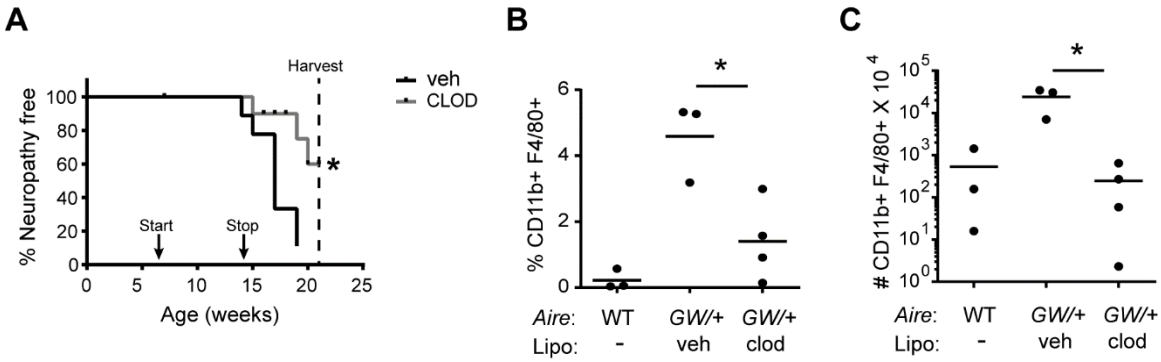

Supplemental figure 17: Macrophages are pathogenic in SAPP. *NOD.Aire* $^{+/+}$ or *NOD.Aire*$^{GW/+}$ mice were treated weekly with vehicle or clodronate-containing liposomes from 7 to 14 weeks of age. Liposome treatment was discontinued due to the development of ascites in clodronate-treated animals. A) Neuropathy incidence curve. B) Frequency and C) number of CD11b+ F4/80+ macrophages in sciatic nerve of vehicle or clodronate treated mice. *p<0.05 by log-rank test (A) or ordinary one-way ANOVA with Tukey's test for multiple comparisons (B, C).

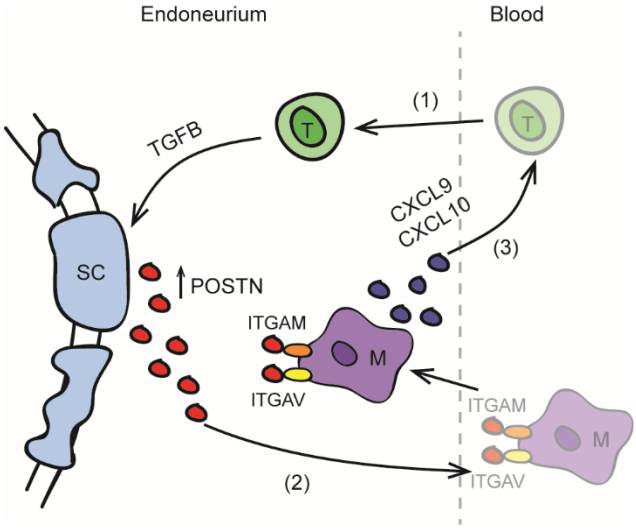

Supplemental figure 18: Schwann cell-derived POSTN promotes SAPP through macrophage recruitment. During SAPP, T cells traffic from the blood into the endoneurium (1). In response to TGFB, Schwann cells upregulate *Postn*, secrete it into the endoneurium, and establish a concentration gradient (2). Upon binding of POSTN to ITGAM or ITGAV, macrophages (M) migrate from the blood into the endoneurium. Macrophages then secrete CXCL9 and CXCL10 (3) to recruit additional T cells to the endoneurium, thus amplifying a positive feedback loop.